AFRL-SN-WP-TP-2006-128

GHz MODULATION OF GaAs-BASED BIPOLAR CASCADE VCSELs (PREPRINT)

**W.J. Siskaninetz, R.G. Bedford, T.R. Nelson, Jr., J.E. Ehret,
J.D. Albrecht, and J.A. Lott**

NOVEMBER 2006

**SENSORS DIRECTORATE
AIR FORCE RESEARCH LABORATORY
AIR FORCE MATERIEL COMMAND
WRIGHT-PATTERSON AIR FORCE BASE, OH 45433-7320**

NOTICE AND SIGNATURE PAGE

This report was cleared for public release by the Air Force Research Laboratory Wright Site (AFRL/WS) Public Affairs Office (PAO) and is available to the general public, including foreign nationals. Copies may be obtained from the Defense Technical Information Center (DTIC) (http://www.dtic.mil).

AFRL-SN-WP-TP-2006-128 HAS BEEN REVIEWED AND IS APPROVED FOR PUBLICATION IN ACCORDANCE WITH ASSIGNED DISTRIBUTION STATEMENT.

PAO Case Number: AFRL/WS 06-0991, 17 Apr 2006.

*//Signature//

WILLIAM J. SISKANINETZ, Electronics Eng.
Photonics Technology Branch
Aerospace Components Division

//Signature//

C. RICHARD LANE, WS Chief
Photonics Technology Branch
Aerospace Components Division

//Signature//

TODD A. KASTLE, Chief
Aerospace Components Division
Sensors Directorate

*Disseminated copies will show "//signature//" stamped or typed above the signature blocks.

REPORT DOCUMENTATION PAGE

Form Approved
OMB No. 0704-0188

1. REPORT DATE *(DD-MM-YY)*
November 2006

2. REPORT TYPE
Journal Article Preprint

3. DATES COVERED *(From - To)*
10/01/2005 – 08/01/2006

4. TITLE AND SUBTITLE
GHz MODULATION OF GaAs-BASED BIPOLAR CASCADE VCSELs (PREPRINT)

5a. CONTRACT NUMBER
In-house

5b. GRANT NUMBER

5c. PROGRAM ELEMENT NUMBER
69199F

6. AUTHOR(S)
W.J. Siskaninetz, R. G. Bedford, and T. R. Nelson, Jr. (AFRL/SNDP)
J.E. Ehret (AFRL/MLPSM)
J.D. Albrecht (AFRL/SNDX)
J.A. Lott (AFIT/ENG)

5d. PROJECT NUMBER
2002

5e. TASK NUMBER
IH

5f. WORK UNIT NUMBER
0C

7. PERFORMING ORGANIZATION NAME(S) AND ADDRESS(ES)

Photonics Technology Branch (AFRL/SNDP)
Aerospace Components & Subsystems Division
Sensors Directorate
Air Force Research Laboratory, Air Force Materiel Command
Wright-Patterson AFB, OH 45433-7320

Materials and Manufacturing Directorate (AFRL/MLPSM)
Air Force Research Laboratory, Air Force Materiel Command
Wright-Patterson AFB, OH 45433

Sensors Directorate (AFRL/SNDX)
Air Force Research Laboratory
Air Force Materiel Command
Wright-Patterson AFB, OH 45433

Air Force Institute of Technology (AFIT/ENG)
Department of Electrical and
Computer Engineering
Wright-Patterson AFB, OH 45433

8. PERFORMING ORGANIZATION REPORT NUMBER
AFRL-SN-WP-TP-2006-128

9. SPONSORING/MONITORING AGENCY NAME(S) AND ADDRESS(ES)
Sensors Directorate
Air Force Research Laboratory
Air Force Materiel Command
Wright-Patterson Air Force Base, OH 45433-7320

10. SPONSORING/MONITORING AGENCY ACRONYM(S)
AFRL-SN-WP

11. SPONSORING/MONITORING AGENCY REPORT NUMBER(S)
AFRL-SN-WP-TP-2006-128

12. DISTRIBUTION/AVAILABILITY STATEMENT
Approved for public release; distribution is unlimited.

13. SUPPLEMENTARY NOTES
This work has been submitted for publication in Optics Letters. This is a work of the U.S. Government and is not subject to copyright protection in the United States.

Accepted for publication in Optics Letters, Optical Society of America publisher. Originally presented at the CLEO/QELS 2006 Conference. PAO Case Number: AFRL/WS 06-0991, 17 Apr 2006.

14. ABSTRACT
The high-frequency modulation characteristics of GaAs-based bipolar cascade vertical cavity surface emitting lasers operating at 980 nm with GaAs tunnel junctions and *p*-doped $Al_{0.98}Ga_{0.02}As$ oxide apertures have been measured. We achieve -3 dB laser output modulations of 6.5 GHz for 2-stage and 9.4 GHz for 3-stage devices in response to small-signal current injection at an operating temperature of -50 °C.

15. SUBJECT TERMS
Semiconductor lasers, Bipolar cascade lasers, Tunnel junctions, Optoelectronics

16. SECURITY CLASSIFICATION OF:			**17. LIMITATION OF ABSTRACT:**	**18. NUMBER OF PAGES**	**19a. NAME OF RESPONSIBLE PERSON** (Monitor)
a. REPORT	**b. ABSTRACT**	**c. THIS PAGE**			William J. Siskaninetz
Unclassified	Unclassified	Unclassified	SAR	10	**19b. TELEPHONE NUMBER** *(Include Area Code)* N/A

Standard Form 298 (Rev. 8-98)
Prescribed by ANSI Std. Z39-18

GHz modulation of GaAs-based bipolar cascade VCSELs

W. J. Siskaninetz

Sensors Directorate, Air Force Research Laboratory & ECE Dept., Air Force Institute of Technology
Wright-Patterson Air Force Base, OH 45433

J. E. Ehret

Materials and Manufacturing Directorate, Air Force Research Laboratory
Wright-Patterson Air Force Base, OH 45433

J. D. Albrecht, R. G. Bedford, and T. R. Nelson, Jr.

Sensors Directorate, Air Force Research Laboratory
Wright-Patterson Air Force Base, OH 45433

J. A. Lott

ECE Dept., Air Force Institute of Technology
Wright-Patterson Air Force Base, OH 45433

Compiled October 25, 2006

The high-frequency modulation characteristics of GaAs-based bipolar cascade vertical cavity surface emitting lasers operating at 980 nm with GaAs tunnel junctions and p-doped $Al_{0.98}Ga_{0.02}As$ oxide apertures have been measured. We achieve -3 dB laser output modulations of 6.5 GHz for 2-stage and 9.4 GHz for 3-stage devices in response to small-signal current injection at an operating temperature of -50 °C.

OCIS codes: 140.5960, 250.7260, 160.6000, 130.0250.

Bipolar cascade (BC) vertical cavity surface emitting lasers (VCSELs) are promising for producing signal gain under high-speed modulation conditions in the radio frequency (RF) range.[1] A particular application of interest is that of RF-photonic links. BC VCSELs that are responsive to GHz injected current modulations can be used as the direct-drive optical signal generation device in such systems, greatly simplifying the component requirements and avoiding the insertion losses associated with external modulators. The central feature of BC devices is the use of reverse-biased tunnel junctions (TJs) to efficiently source electron and hole currents to multiple active regions by recycling the valence band electrons resulting from optical recombination. Benefits of BC designs over typical *p-i-n* diode lasers include greater quantum efficiencies that can exceed unity when using multiple stages,[2] improved RF impedance matching through increased series resistance,[3] and reduced noise figures as a result of uncorrelated carrier recycling among stages.[4]

Even though high-frequency performance is crucial, few reports of measured BC laser modulation data exist. Despite significant advances in InP- and GaAs-based BC VCSEL structures and their extensive characterizations,[5–8] to date we have located only the high-frequency analysis reported by Knödl, et al.[9] wherein modulated current efficiency factors are extracted from relative intensity noise measurements as a means of high-frequency characterization.

In this Letter, high-frequency measurements of modulated laser light output as a function of RF small-signal injected current for a series of BC VCSELs are reported. First we present the details of the growth and fabrication of GaAs-based BC VCSELs with operating wavelengths $\sim$ 980 nm. Next, we present and discuss measured laser characteristics including light power and voltage versus injected current (LI and VI) and small signal laser modulation results approaching 10 GHz at a temperature of -50 °C.

A schematic for a single-stage laser structure, Fig. 1a), a micrograph of a fabricated high-speed device, Fig. 1b), and a close-up scanning electron microscope (SEM) image of the VCSEL aperture, Fig. 1c), are shown. The BC VCSELs were grown on n^+ GaAs substrates by molecular beam epitaxy. The laser cavities consist of 1-, 2-, or 3-stage $\frac{5}{2}\lambda$ microcavities, each containing a graded p-doped $Al_{0.98}Ga_{0.02}As$ oxide aperture (OA) and a GaAs TJ positioned at longitudinal nodes of the optical standing wave, and a triple quantum well (QW) active region placed at an antinode.

The following description gives the layer structure for a 1-stage device. The top distributed Bragg reflector (DBR) consists of 15 abrupt $GaAs/Al_{0.90}Ga_{0.10}As$ pairs, Si-doped at 4×10^{18} cm^{-3}. The microcavity is formed from the top DBR as follows (numbering scheme is indicated in Fig. 1a). First, an undoped GaAs spacer layer *(1)* is used to center a TJ *(2)* at the first node. The TJ, reported previously,[10] consists of a Si δ-doped GaAs layer and a C-doped GaAs layer, each TJ layer is 200 Å thick. Below this, an undoped GaAs spacer layer *(3)* positions an OA region *(4)* at the next node of the standing wave. The 300 Å thick OA is p-type $Al_{0.98}Ga_{0.02}As$ and has graded transition layers on either side. Under the OA is an approximately $\frac{3}{4}\lambda$ thick undoped GaAs spacer layer *(5)* designed to place the active region in an antinode. The active region *(6)* consists of three 80 Å thick $In_{0.20}Ga_{0.80}As$

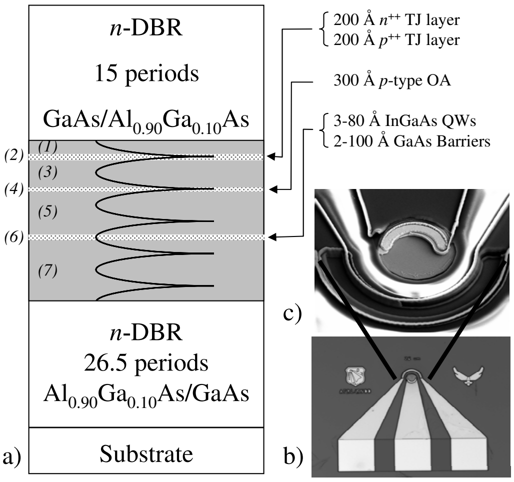

Fig. 1. a) Schematic of a single-stage BC VCSEL. The curve indicates the optical field of the $\frac{5}{2}\lambda$ cavity resonance. The insets show b) a micrograph of a processed high-speed device and c) a close-up SEM image of the VCSEL aperture.

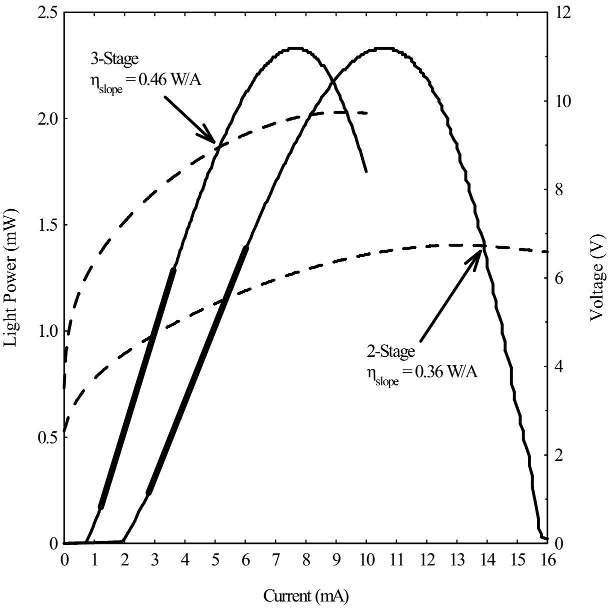

Fig. 2. LI and VI characteristics for a 3-stage and a 2-stage device at -50 °C. The solid lines are the LI characteristics and the dashed lines are the VI characteristics. The heavy line portions of the LI curves indicate the linear regime where the slope efficiencies were calculated.

wells separated by 100 Å thick GaAs barriers. Finally, an undoped GaAs layer *(7)* approximately 1-λ thick is used to complete the cavity. For 2- and 3-stage structures the entire microcavity is repeated. The bottom DBR consists of 26.5 abrupt $Al_{0.90}Ga_{0.10}$As/GaAs pairs with the same layer thicknesses and doping as the top DBR.

Top-contacted, mesa-isolated BC VCSELs with 10 to 50 μm circular mesas were fabricated. Semi-ring annuli ohmic top contacts were formed lithographically and contact metal (Ni-Ge-Au-Ni-Au) was evaporated onto the patterned topside. The mesa dry etch was stopped on the third GaAs layer of the bottom DBR, just below the cavity as determined by in-situ reflectivity. The bottom contact was patterned and the same metals were deposited on both the patterned side and the backside (for thermal contact). The contacts were annealed in forming gas at 410 °C for 15 s. The OAs were formed with an in-situ oxidation furnace at 400 °C for four hours, yielding an approximate 10 μm oxide penetration depth. The annealing step was performed to allow for preoxidation device characterization. The anneal and subsequent oxidation did not affect the quality of the ohmic contacts. Next, a 5,000 Å thick Si_3N_4 layer was deposited for electrical isolation and sidewall passivation, followed by a 5 μm layer of SU-8 used for planarization. The mesas and bottom contacts were opened lithographically and the uncovered Si_3N_4 was subsequently dry etched with Freon 23-O_2 (40 sccm-2 sccm) to completely clear out the mesa aperture and the electrical contacts. The ground-signal-ground (g-s-g) cascade contact pads were lithographically defined and Ti - Au layers were sputtered to ensure step coverage.

In preparation for high-frequency characterization we determined the operating conditions and biasing properties of the lasers. LI and VI characteristics for 1-, 2-, and 3-stage BC VCSEL devices were measured at various temperatures. Figure 2 shows the CW LI (solid lines) and VI (dashed lines) characteristics for a 3-stage and a 2-stage BC VCSEL at -50 °C. The test system consisted of an environmentally controlled probe station and an HP-7145A semiconductor parameter analyzer (SPA) connected to a g-s-g microprobe. A 1 cm diameter Si detector with a 5% neutral density filter was used to collect the output light.

The "electron recycling" benefit of the BC VCSEL structure is immediately obvious by comparing the 2- and 3-stage LI data. The increased round trip gain from the additional stage (without a proportional increase in current) manifests in a rise in slope efficiency, η_{slope} from 0.36 W/A for the 2-stage device to 0.46 W/A for the 3-stage device, as well as the reduction in the threshold current from 1.9 mA for the 2-stage device to 0.7 mA for the 3-stage device. The 1-, 2- and 3-stage devices all lased at -50 °C. The single-stage devices, however, did not yield measurable frequency responses, due primarily to low gain resulting from inadvertent cavity detuning relative to the gain peak and from small round-trip gain resulting from the low number of DBR pairs and only three QWs. Additionally, this detuning results in degraded CW performance of BC VCSELs at higher temperatures.

High-frequency laser modulation response measurements were performed at the same temperatures along several bias points along the positive slope of the LI curves. The output modulation was determined using the s-parameters obtained from an HP-8720A microwave network analyzer (MNA). The test system consists of a stable DC current source connected to the Port-1 bias-tee of the MNA. The MNA applies a -10 dBm (0.1 mW) small-signal modulation onto the laser bias. The signal was supplied to the VCSEL by a high-speed coaxial cable connected to the microprobe. The modulated light output was collected using a 63 μm core multimode fiber and detected using a 25 GHz high-speed detector. The output signal from the detector was returned to port 2 of the MNA via another high-speed coaxial cable.

Fig. 3 shows the device frequency response, which is proportional to the MNA measured $|s_{21}|$, for 28 μm diameter mesas corresponding to 8 μm apertures, as described in the previous section. These devices were chosen because of superior performance and single-mode output as determined by imaging the near field. Taken in context, the measured performance data reported here were the best values obtained when the laser modulation experiment was repeated for devices with mesa/OA diameters equal to 28/8, 30/10, 35/15, and 40 μm/20 μm at -50 °C to +25 °C.

In order to compare independent measurements to a common -3 dB standard, the data points in Fig. 3 have been scaled by plotting 10 $log\,[|s_{21}|/MTF(0)]$ where MTF is the two-pole modulation transfer function. The two-pole form takes into consideration the low-frequency parasitic peak that was often observed. In Fig. 3, the 2-stage device shows the effects of a low-frequency parasitic response. The functional form for the fitting was

$$MTF(\omega) = \sqrt{\frac{A+B+C}{(1+\tau_{par}^2\omega^2)[\gamma^2\omega^2+(\omega^2-\omega_r^2)^2]}} \qquad (1)$$

where

$$\begin{aligned} A &= C_m^2(1+\tau_{par}^2\omega^2)\omega_r^4 && (2)\\ B &= 2C_mC_{par}\omega_r^2[(\gamma\tau_{par}-1)\omega^2+\omega_r^2] && (3)\\ C &= C_{par}^2[\gamma^2\omega^2+(\omega^2-\omega_r^2)^2]. && (4) \end{aligned}$$

The angular frequency is ω, ω_r is the relaxation oscillation frequency, γ is the damping factor, C_m is the single pole MTF amplitude constant, C_{par} is the parasitic amplitude constant, and τ_{par} is the parasitic time constant. Disentangling the parasitic effects is outside the scope of this letter.

The frequency responses for a 3-stage and a 2-stage device are shown in Fig. 3. The MTF curves correspond to fits with $f_r \equiv \omega_r/2\pi = 4.78$ and 6.26 GHz and $\gamma = 5.63$ and 7.45 GHz for the 2-stage and 3-stage measurements, respectively. The 3- and 2-stage BC VCSEL devices exhibit frequency responses of 9.3 GHz and 6.5 GHz, respectively at the labeled biasing conditions. The 3-stage device at +25 °C does operate under small-signal modulation but with a lower 4.0 GHz -3 dB response. However, the modulation peak is quite sharp, indicating further current injection would increase the -3 dB frequency bandwidth. Unfortunately, the modulation signal falls off at higher bias currents because the laser is operating near the maximum of its positive LI slope. Further increase in current reduces the -3 dB frequency response as the laser operation begins to degrade due to heating effects and increasing gain-cavity mismatch.

We have demonstrated GHz operation of BC VCSELs at an operating temperature of -50 °C. While these BC VCSELs do operate at room temperature, improvements such as compositionally grading the DBR mirror layers and optimizing the gain peak vs. cavity tuning overlap should dramatically improve room temperature operation. Room temperature BC VCSELs operating greater than 10 GHz with high slope efficiencies is achievable.

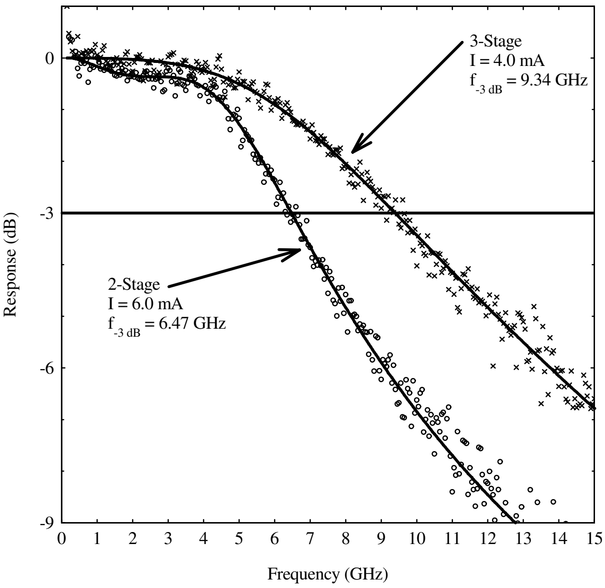

Fig. 3. Frequency response characteristics for BC VCSELs at -50 °C operating at the labeled conditions. The data points are measured $|s_{21}|$ values normalized to $MTF(0)$ and the curves are normalized MTFs.

The authors would like to thank J. Breedlove, P. Cassity, D. Cathcart, and L. Callahan of Wyle Laboratories for their technical support. WJS also thanks the Dayton Area Graduate Studies Institute for their support. This work was supported in part by the Air Force Office of Scientific Research.

References

1. S. Patterson, G. Petrich, R. Ram, and L. Kolodziejski, Elect. Lett. **35**, 395 (1999).
2. T. Knödl, M. Golling, A. Straub, and K. Ebeling, Elect. Lett. **37**, 31 (2001).
3. J. Getty, E. Skogen, L. Johansson, and L. Coldren, IEEE Photon. Tech. Lett. **15**, 1513 (2003).
4. P. Mayer, F. Rana, and R. Ram, Appl. Phys. Lett. **82**, 689 (2003).
5. J. Wierer, P. Evans, N. Holonyak, and D. Kellogg, Appl. Phys. Lett. **71**, 3468 (1997).
6. W. Schmid, D. Wiedenmann, M. Grabherr, R. Jager, R. Michalzik, and K. Ebeling, Elect. Lett. **34**, 553 (1998).
7. J. Kim, E. Hall, O. Sjölund, G. Almuneau, and L. Coldren, Elect. Lett. **35**, 1084 (1999).
8. R. Koda, C. Wang, D. Lofgreen, and L. Coldren, Appl. Phys. Lett. **86**, 211104 (2005).
9. T. Knödl, M. Golling, A. Straub, R. Jager, R. Michalzik, and K. Ebeling, IEEE J. Select. Topics Quantum Electron. **9**, 1406 (2003).
10. W. Siskaninetz, J. Ehret, J. Lott, J. Griffith, and T. Nelson, Appl. Phys. Lett. **86**, 111108 (2005).